Chinese Chemical Letters 35 (2024) 108361

Contents lists available at ScienceDirect

Chinese Chemical Letters

journal homepage: www.elsevier.com/locate/cclet

Size-dependent macrophage-targeting of mannose-modified rosiglitazone liposomes to alleviate inflammatory bowel disease

Erjin Wang[a,1], Run Han[a,1], Mingyue Wu[a], Yuan He[b], Yaxin Cheng[a], Jiahong Lu[a,c,d,*], Ying Zheng[a,c,*]

[a] State Key Laboratory of Quality Research in Chinese Medicine, Institute of Chinese Medical Sciences (ICMS), University of Macau, Macau 999078, China
[b] Department of Pharmacy, Xuzhou Medical University, Xuzhou 221004, China
[c] Faculty of Health Sciences, University of Macau, Macau 999078, China
[d] Guangdong-Hong Kong-Macau Joint Lab on Chinese Medicine and Immune Disease Research, University of Macau, Macau 999078, China

ARTICLE INFO

Article history:
Received 30 December 2022
Revised 19 March 2023
Accepted 20 March 2023
Available online 22 March 2023

Keywords:
Macrophage targeting
Liposome
Mannose
Particle size
Inflammatory bowel disease

ABSTRACT

Inflammatory bowel disease (IBD) is a refractory chronic intestinal inflammatory disease caused by a malfunction of immune system. As the key immune cells in the intestine, macrophages play an important role in maintaining intestinal homeostasis and tissue repair of the IBD. Pharmacological modulation of macrophage function exhibits the promising therapeutic effect for IBD. In this study, mannose-modified liposomes (MAN-LPs) are prepared for macrophage targeting to improve therapeutic efficiency. Rosiglitazone (ROSI) as an agonist of peroxisome proliferators-activated receptor γ (PPAR-γ) is used as the model drug to fabricate different sized liposomes. The impacts of mannose modification and particle size for macrophage targeting are investigated in cells, zebrafish, and mouse models and the therapeutic effects of the MAN-LPs are evaluated on dextran sulfate sodium (DSS)-induced IBD mouse. Compared to unmodified liposome, MAN-LPs display higher uptake by RAW 264.7 cells and better co-localization with macrophage in zebrafish model. Furthermore, MAN-LPs could effectively accumulate in the inflammatory intestinal sites in IBD mouse model. Most importantly, the targeting ability of MAN-LPs is obviously enhanced with the increasing of particle size, whereas the largest MAN-LPs particles achieve the best anti-inflammatory effect in cells, and a higher therapeutic efficiency in IBD mouse model. Therefore, mannose-modified liposome is a promising strategy for macrophage-targeting in IBD treatment. Particle size of MAN-LPs will affect macrophage targeting ability, as well as the therapeutic effect *in-vivo*.

Inflammatory bowel disease (IBD) is a group of chronic non-specific intestinal inflammatory diseases, including ulcerative colitis (UC) and Crohn's disease (CD), that has been developed as a global health problem with continuous growth of incidence rate [1,2]. It is an intestinal related disease with the symptoms of recurrent and persistent abdominal pain, weight loss, diarrhea, and mucous bloody stool that severely restrict the quality of life [3]. Although the pathogenesis of IBD is not very clear, it can be confirmed that many factors including intestinal immunity, gut microorganisms and exotic stimulants commonly influence the homeostatic imbalances in enteric [4]. The chronic inflammatory features include the impairments of intestinal epithelial barrier and the imbalance of immune regulation in colon and rectum sites, so promoting the resolution of intestinal inflammation and mucosal repair is critical for the treatment of IBD. Currently, 5-aminosalicylic acid (5-ASA) is the first line drug for IBD treatment in clinic, and corticosteroids like prednisolone and budesonide are the main strategy for clinical therapy [5]. Biological drugs and immunotherapy agents such as infliximab, adalimumab and golimumab that could bind to and neutralize tumor necrosis factor-α (TNF-α) have also been developed and applied for relieving inflammation [6]. However, due to the low targeting of conventional 5-ASA, corticosteroids and immunotherapy agents, patients are subjected to long-term treatment with high doses of drugs with severe systemic side effects [7]. Therefore, the targeted drug delivery platform is urgent to be explored and developed for IBD therapy.

With the development of nanotechnology and biotechnology, various nanoparticles are delivered into the inflammatory colon

* Corresponding authors at: State Key Laboratory of Quality Research in Chinese Medicine, Institute of Chinese Medical Sciences (ICMS), University of Macau, Macau 999078, China.
E-mail addresses: jiahongLu@umac.mo (J. Lu), yzheng@umac.mo (Y. Zheng).
[1] These authors contributed equally to this work.

https://doi.org/10.1016/j.cclet.2023.108361
1001-8417/

site by passive and active targeting effects [7,8]. Due to the enhanced permeability and retention (EPR) in the destroyed intestinal epithelial tissue, nanoparticles that based on specific physical properties could deliver and accumulate into the inflamed colon to increase drug concentrations [9]. For example, Abhijit *et al*. has reported a budesonide nano-suspensions to improve penetration efficiency in intestinal tissue by tailing particle size (~225 nm) and muco-inert coating materials [10]. Zhang *et al*. have constructed a smart cauliflower-liked nanoparticle to transport astaxanthin into the colon, which achieved pH-dependent release to enhance biological activities [11]. Active targeting is mostly relying on receptor-mediated delivery systems. As the pathophysiological conditions have been changed in IBD, many signals including receptors and proteins are overexpressed on the epithelia cells and immune cells, which are the promising targets. CD44 is the receptor of hyaluronic acid (HA) that express on the surface of various cells and response for cell interaction, adhesion and migration. A methylcellulose and HA cross-linked hydrogel coating bovine serum albumin has been prepared for rectal delivery with great therapeutic effect. A diselenide-bridged HA nanoparticles could effectively reduce reactive oxygen species (ROS) to realize antioxidant relieving colitis [12,13]. Except that, folate receptor, transferrin receptor and cell adhesion molecules are the potential targets to improve biological activities. Compared with the traditional forms, targeted drug delivery systems have demonstrated superior properties in treating IBD with higher efficiency and lower side effects.

During the process of IBD progression, macrophages play an important role in intestinal immune homeostasis and prevention of excessive immunity [14]. Under physiological conditions, intestinal macrophages exhibit a relatively inert phenotype, thereby avoiding inappropriate inflammatory and activating immune responses. In the state of IBD, a large number of pro-inflammatory mediators are produced, and inflammatory cytokines are released that disrupt the gut microbial environment, resulting in mucosal structural destruction and immune dysregulation. Macrophage polarization is critical for inflammation process that is closely related with initiating, maintaining and resolving of inflammation [15]. As the innate immune cells in gut, the function of macrophages is essential for IBD pathological progression [16]. Therefore, many drug therapies improve IBD symptoms by acting on macrophages to inhibit inflammatory signaling pathways or to induce polarization of macrophage phenotypes [17,18]. Peroxisome proliferators-activated receptor γ (PPAR-γ) is expressed on macrophage, which is regarded as a promising macrophage-targeted receptor for IBD treatment. It has been reported that PPAR-γ could induce macrophage polarize as M2 phenotype and accelerate the recovery from IBD [19]. Rosiglitazone (ROSI), a synthetic agonist for PPAR-γ, has been used for the treatment of type 2 diabetes in clinic, also developed to suppress the inflammation in IBD by inhibiting macrophage inflammatory response [20,21]. However, increasing drug accumulation in the inflammatory site and avoiding systemic side effect are still a challenge for further clinical application [22,23].

Mannose receptor (MR) is an endocytic receptor involved in homeostasis and immunity that highly expressed on macrophage. It has reported that mannose modified trimethyl chitosan-conjugated nanoparticles could selectively deliver to intestinal macrophage by combining with mannose receptors for mucosal repair and immunomodulation [24]. Nanoparticles functionalized with mannose have been applied for anti-tumor and anti-inflammation treatment, which proved the feasibility of mannose for macrophage targeting [25,26]. This study will design a ROSI loaded mannose-modified liposome (MAN-ROSI-LP) that target to inflammatory macrophages to precisely deliver drugs into the intestinal inflammation site for IBD treatment. Moreover, the size effect for liposome particle targeting is also explored to achieve the best drug accumulation in colon site to take anti-inflammation function. As the transparent and dynamic *in-vivo* model, zebrafish is more and more recognized for nanoparticle bio-fate study in drug discovery [27]. To directly view the bio-distribution of the liposomes, zebrafish provides a new platform for tracking particles *in vivo*. Therefore, the performance of MAN-ROSI-LPs with different sizes were investigated both *in-vitro* and *in-vivo* to enhance drug accumulation in the GI tract and then improve therapeutic efficiency for IBD treatment. All the zebrafish experiments were performed according to the protocol approved by the Animal Research Ethics Committee of the University of Macau (ethics number: UMARE-021–2018).

To investigate the size effect of the MAN-ROSI-LPs on macrophage targeting, a series of liposomes were prepared with different sizes as shown in Fig. 1A, while polyethylene glycol (PEG)-ROSI-LP without mannose modification was also prepared for comparison. The hydrodynamic diameter of PEG-ROSI-LP was 114.4 ± 9.89 nm, while that of small (S-MAN-ROSI), medium (M-MAN-ROSI) and large (L-MAN-ROSI) liposomes was 124.6 ± 10.45 nm, 219.8 ± 15.68 nm and 324.5 ± 22.75 nm, respectively (Fig. 1B). Transmission electron microscopy (TEM) images demonstrated all the prepared liposomes were spherical particles without aggregation or break. The polydispersity index (PDI) of each sample was within 0.2, which confirmed the homogeneity of liposome particles (Fig. 1C). After 7 days storage at 4 °C, there were no obvious changes for particle size, indicating the good stability during the short storage period (Fig. 1D). PEG- and MAN-ROSI-LPs were all neutral charged with zeta potential of around 0.1. Free ROSI were separated from the liposome solution after ultrafiltration process, and the calculated encapsulation efficiency of the PEG-ROSI-LP, S-, M- and L-MAN-ROSI were 78.8%, 88.8%, 83.2% and 82.8%, respectively. The dissolution behavior of the free drug and liposomes were measured as shown in Fig. 1E, where free drug and liposomes demonstrated the similar dissolution properties. About 20% free drug was released into the medium within 1 h, then quickly dissolved in the next 8 h and reached to the maximal release at 24 h For the dissolution of PEG-ROSI-LP, there were 25% drug released at 1 h and reached to 90% at 8 h Similarly, all three sized MAN-ROSI-LPs showed the comparable release profiles. S-MAN-LP exhibited a relatively quick release that fully dissolved at 8 h, whereas M- and L-MAN-LPs gradually released and reached to 100% dissolution after 24 h.

To verify the targeting effect of mannose modified liposome for macrophages, the fluorescent dye DiI was used as a marker to label liposomes, while PEG-LP was used as the comparison. After co-cultured with liposomes for 2 h, the fluorescence intensity (FI) of the cell lysate was detected with a microplate reader as shown in Fig. 2A. The FI of RAW 264.7 cell lysate in each MAN-DiI-LP group was markedly higher than that in PEG-DiI-LP ($P < 0.05$), and the FI gradually increased as the liposome particle size increased. Conversely, for the epithelial cell A549 lysate, there were no noticeable difference of FI between mannose modified groups and PEG-DiI-LP, and no particle size dependent effect under the same conditions. The FI of single cell that measured by flow cytometer exhibited the similar results (Fig. 2B). To study whether the higher uptake of MAN-DiI-LPs was attributed to the specific targeting with mannose receptor, RAW 264.7 was pre-treated with D-mannose (a competitive agent of mannose receptor) for 1 h and then co-cultured with the liposomes for 2 h. The FI for each sample was measured by flow cytometry as shown in Fig. 2C. For mannose modified liposome, D-mannose could inhibit the particle uptake by macrophage as the FI were obviously reduced with mannose pretreatment, especially for large particles. Whereas the uptake of unmodified liposome did not show difference with or without D-mannose pretreatment group, indicating that there was no competition between mannose and normal liposome. These results

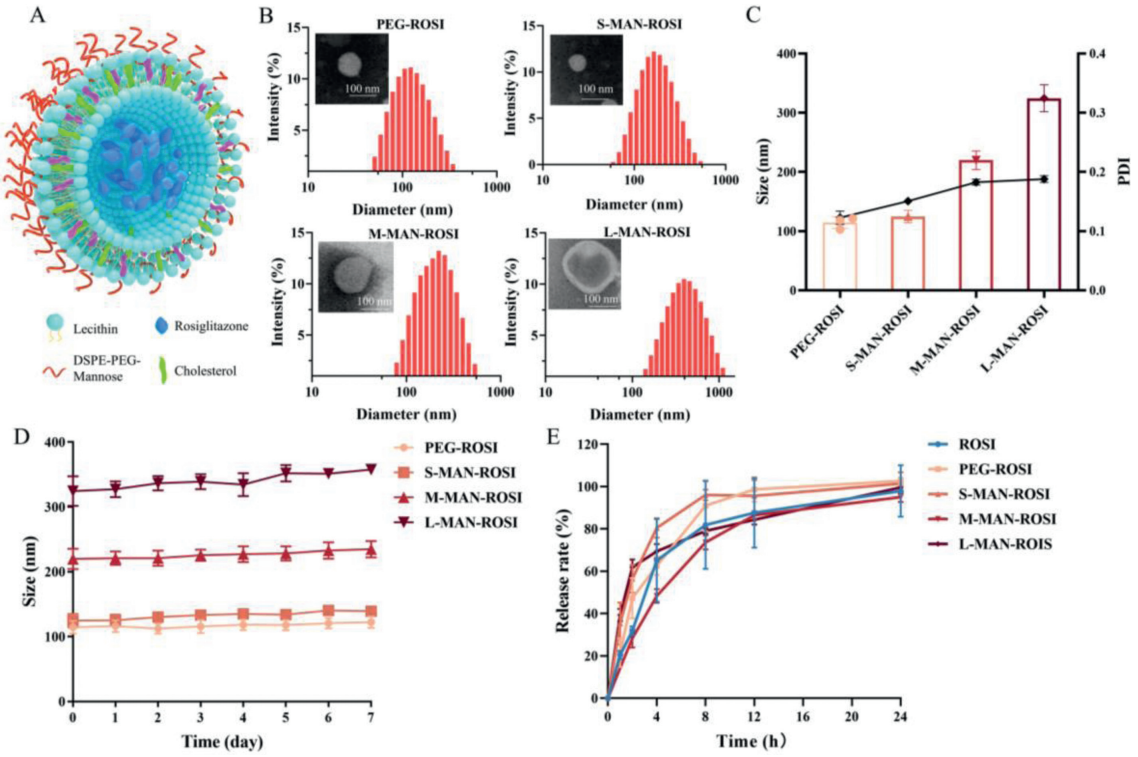

Fig. 1. Characterization of the MAN-ROSI-LPs. (A) The schematic of MAN-ROSI liposome particle. (B) The size distribution and representative TEM images of PEG-ROSI and small, medium, large MAN-ROSI liposomes (the scale bar is 100 nm). (C) The size and PDI of liposomes. (D) The particle size change of PEG- and MAN-ROSI-LP stored at 4 °C during 7 days. (E) *In-vitro* release rate of the free drug, PEG- and MAN-ROSI-LPs in PBS with 1% Tween 80 within 24 h. Data are shown as mean ± standard deviation (SD) ($n = 3$).

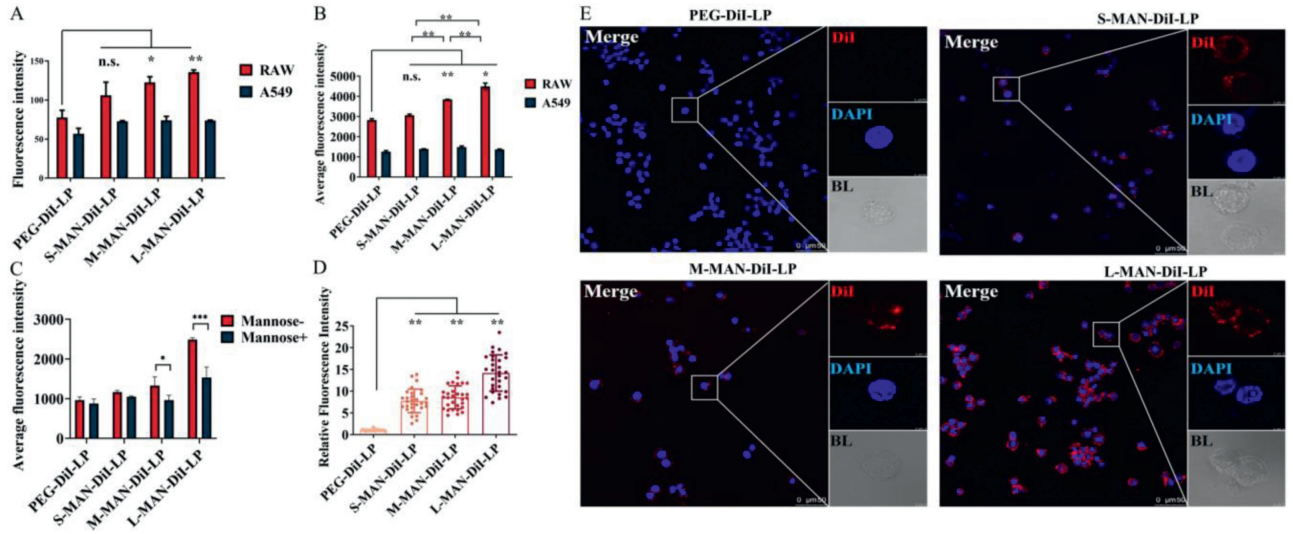

Fig. 2. The targeting effect of mannose-modified liposome to macrophages *in vitro*. RAW 264.7 and A549 cells were treated with PEG-DiI-LP and MAN-DiI-LP with different particle sizes containing the same concentration (25 μg/mL) of DiI for 2 h. (A) Cells were lysed with RIPA and the lysates DiI fluorescence intensity were detected by microplate reader at $\lambda = 565$ nm ($n = 3$). (B) Cells were digested with trypsin, and the fluorescence intensity of each cell was detected by flow cytometry ($n = 3$). (C) The intracellular uptake of PEG-DiI-LP and different size MAN-DiI-LP with or without mannose pretreatment. (D) 30 cells were randomly selected from each group and the fluorescence intensity was quantitatively analyzed by LAS-X software. (E) Cells were fixed with paraformaldehyde, and the phagocytosis of different liposomes was observed by confocal microscope. DiI was marked in red and macrophage nuclei are stained with DAPI (blue). All significant differences of MAN-DiI-LPs compared with PEG-DiI-LP were determined by one-way ANOVA. Data are shown as mean ± SD (n.s., no statistical difference. $^{*}P < 0.05$, $^{**}P < 0.01$).

suggested that mannose modified liposome could effectively target to macrophage by combining with mannose receptors and improve the particle delivery efficiency. Furthermore, the uptake of liposomes by RAW 264.7 was also directly observed by confocal microscopy shown in Fig. 2E. After 2 h incubation, there were almost no PEG-DiI-LPs uptake by macrophage. However, RAW 264.7 cells co-cultured with L-MAN-DiI-LPs showed more obvious fluorescence co-localization compared with that of S- and M-MAN-DiI-LPs, suggesting that larger liposomes were easily uptake by macrophages. Thirty cells in each group were randomly selected for quantitative analysis, which also confirmed the uptake of MAN-DiI-LP was more than PEG-DiI-LP with statistical differences, where

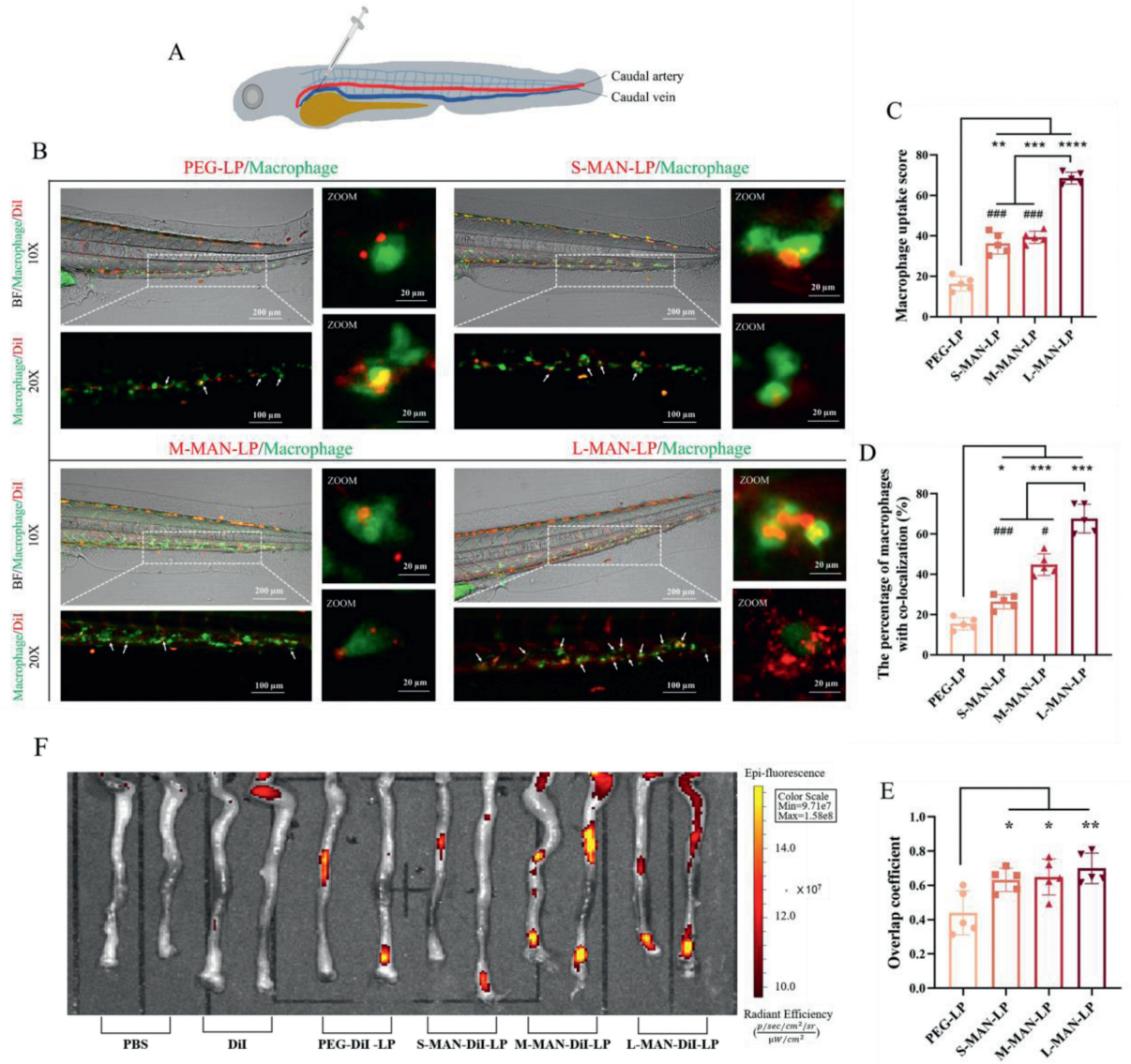

Fig. 3. The biodistribution of PEG-DiI and MAN-DiI liposomes in 2 dpf *Tg* (*mpeg1: EGFP*) zebrafish larvae and IBD mouse model. (A) The schematic of vein injection in zebrafish. (B) The co-localization of macrophage and DiI liposomes in 12 h after injection. (C) Macrophage uptake score of PEG-DiI and MAN-DiI-LPs by macrophage. (D) The percentage of macrophages that co-localized with PEG-DiI and MAN-DiI-LPs. (E) Overlap coefficient of each group that co-localized with macrophage. The macrophage of zebrafish was labeled as green fluorescence and liposome particles were labeled as red fluorescence. (F) Before induction of colitis, mice were randomly divided into six groups ($n = 3$): negative control group (PBS), free DiI group (DiI), small particle size vehicle-treated group (PEG-DiI- LP) and three MAN-DiI-LP groups with different particle sizes (S-MAN-DiI-LP, M-MAN-DiI-LP and L-MAN-DiI-LP). After drinking 3.5% DSS for 5 days, 100 μL different solutions with 1 μg/mL DiI were injected into the tail vein. The animal imager was used to observe the fluorescence signal intensity of the isolated intestine after treatment for 24 h. All images were observed by CLSM at 24 hpi. Significant differences of MAN-DiI-LPs compared with PEG-DiI-LP were determined by one-way ANOVA. Data are shown as mean ± SD ($n = 5$, $^{*}P < 0.05$, $^{**}P < 0.01$, $^{***}P < 0.001$, $^{****}P < 0.0001$ compared with PEG-LP group; $^{\#}P < 0.05$, $^{\#\#\#}P < 0.001$ compared with L-MAN-LP group).

the uptake of the large particles was significantly higher than those of the small and medium particles (Fig. 2D).

The *in-vivo* size-dependent macrophage-targeting of mannose modified liposomes were further explored in the *Tg* (*mpeg1: EGFP*) zebrafish that had the enhanced expression of green fluorescence protein on vascular macrophage. As shown in Figs. 3, the confocal laser scanning microscope (CLSM) images of zebrafish exhibited the fluorescence co-localization of macrophage with PEG- and MAN-LPs. Firstly, DiI labeled liposome particles were injected into vein as illustrated in Fig. 3A. After 24 h post injection (hpi), the particle distribution in vascular was presented in Fig. 3B. There were very little PEG-LP particles uptake by macrophage, whereas the red fluorescence of MAN-LPs overlapped with green fluorescence were brighter, which suggested mannose modified liposomes could effectively target to macrophage. Moreover, with the particle size increasing, the co-localization of green and red fluorescence was more obvious. From the perspective of signal macrophage that co-localized with liposome particles, macrophage uptake score, the percentage of macrophages with co-localization and overlap coefficient of different liposome treatment groups were calculated to semi-quantitatively evaluate co-localization as shown in Figs. 3C–E. Macrophage uptake score in MAN-LPs groups were higher than PEG-LPs, especially for L-MAN-LP that was significantly higher than other groups. The percentage of the macrophages that were co-localized with liposome particles to total macrophages in whole zebrafish was showed in Fig. 3D, where the co-localized macrophage in L-MAN-LPs was also larger than those of the PEG-LP, S- and M-MAN-LPs. The overlap coefficient was also analyzed in Fig. 3E. Consistently, it was obvious that overlap coefficient of MAN-LPs was higher than PEG-LP, especially for the L-MAN-

LP group which exhibited significant differences with that of the PEG-LP. Therefore, mannose modified liposomes mostly tended to aggregate around macrophage and could be effectively uptake by macrophage *in vivo*. Moreover, this targeting effect was significantly enhanced with the increased particle size.

Whether the MAN-LPs could be delivered and accumulated in the inflammatory sites in IBD model, the dextran sulfate sodium (DSS)-treated mice model that reproduced the symptoms of human ulcerative colitis were used in this study [28]. All mouse breeding and experimental procedures were approved by the Animal Experiment Ethics Committee of the University of Macau (ethics number: UMARE-023–221). After adding DSS into free drinking water to induce IBD mice model, the gradual onset of IBD-related pathological symptoms, including body weight loss, blood in the stool, rectal bleeding, and pathological changes in colonic sections, were obviously observed in mice from 1 day to 6 days. On the last day of DSS administration, PBS, free DiI, PEG-DiI-LPs and MAN-DiI-LPs with different particle size were injected through the tail vein. After 24 h, the whole intestines of mice were photographed with *in-vivo* imaging. As shown in the Fig. 3F, more MAN-DiI-LP particles accumulated in the colon where was the most severely inflammatory site of IBD, indicating that mannose could effectively target macrophages and accumulate in inflammatory tissue. Furthermore, as the particle size increased, the fluorescence intensity of the colon tissue gradually enhanced, indicating that the larger particles enhanced targeting of MAN-DiI-LPs to the inflammatory sites *in-vivo*. Then macrophages in colon were labeled as maker F4/80 and colon tissue slices were photographed by fluorescence confocal microscope. The MAN-DiI-LPs showed the obvious co-localization with macrophages, especially for larger particles (Fig. S2 in Supporting information), which was consistent with the overall distribution in colon and further confirmed the better co-localization of MAN-DiI-LPs.

In the inflammatory site of colitis, macrophage could be activated and polarized as M1 phenotype, some pro-inflammatory cytokines were produced and released to enhance the severity of inflammation. After the treatment of MAN-ROSI-LPs, the inflammatory cytokines of macrophage were measured to verify the macrophage targeting ability and anti-inflammatory effect of MAN-ROSI-LPs. RAW 264.7 was firstly induced by lipopolysaccharides (LPS) to build the inflammatory cell model. With the LPS and MAN-ROSI-LPs co-cultured, the mRNA level of cytokines was measured by RT-PCR (Figs. S3A–C in Supporting information). It was clear that mRNA levels of inducible nitric oxide synthase (iNOS), interleukin-1β (IL-1β) and IL-6 were significantly up-regulated after LPS stimulation and could be inhibited by free ROSI. But PEG-ROSI-LP did not show the ability to attenuate the up-regulation of inflammatory factor transcription induced by LPS. In the MAN-ROSI-LP groups, the mRNA levels of iNOS, IL-1β and IL-6 decreased with the increase of particle size, and gradually tended to the effect of free ROSI. Next, the secretion of inflammatory factors in the cell culture supernatant was examined by enzyme-linked immunosorbent assay (ELISA). MAN-ROSI-LPs could effectively decrease the release of IL-6 induced by LPS compared with PEG-ROSI-LP (Fig. S3D in Supporting information). Moreover, with the size increased, less IL-6 was released. Similarly, MAN-ROSI-LPs also inhibited the produce of IL-1β, especially the L-MAN-ROSI obviously decreased the concentration of IL-1β in cell culture supernatant (Fig. S3E in Supporting information). For the anti-inflammatory cytokine of IL-10, ROSI could stimulate the production of IL-10, and the L-MAN-ROSI significantly improved the express level of IL-10 (Fig. S3F in Supporting information). Inhibiting pro-inflammatory cytokines and promoting anti-inflammatory cytokines could synergistically mitigate inflammation with MAN-ROSI-LPs treatment.

Because the large sized liposomes demonstrated the best targeting ability, L-MAN-ROSI-LP was selected for the follow-up *in-vivo* bioactivity experiments. The timeline of building IBD mouse model was described in Fig. 4A. Following the inducement of IBD by 3.5% DSS water, ROSI of 0.2 mg/kg or the equal concentration of ROSI encapsulated in L-MAN-ROSI-LP was injected into the tail vein every day. On the 6th day of the experiment, DSS was changed to the free drinking water to observe the recovery of IBD symptoms in different group of mice. Disease activity index (DAI) was used to evaluate the severity of the disease in mice. The higher of the score, the more severe of IBD. As shown in Fig. 4B, except the control group (the normal water drinking group), the DAI of the other groups continuously increased from 1 day to 8 days. During DSS inducing, ROSI slightly reduced DSS-induced DAI levels compared with the model group, although no statistical difference. Whereas the treatment of MAN-ROSI-LP effectively reduced the DAI of mice compared with the model and ROSI groups ($P < 0.05$). After the DSS inducing, the model group exhibited the further aggravation of the disease due to the lack of effective treatment. Conversely, DAI decreased in both the ROSI and L-MAN-ROSI-LP groups but was more pronounced in the L-MAN-ROSI-LP, as indicated by an upward trend in body weight, better stool morphology, and no apparent bleeding.

After 8 days, mice were sacrificed, and the colon was taken to measure the length. The results showed that the colon length of L-MAN-ROSI-LP treatment mice group was significantly longer than that of free ROSI and control group (Figs. 4C and D). On the other hand, L-MAN-ROSI had no significant effect on the liver and spleen index of the mice (Figs. 4E and F). HE staining of colon sections showed that the colon tissue of animals in the model group exhibited strong mucosal erosion, shortened crypts, accompanied by inflammatory cell infiltration, edema and marked thickening of the intestinal wall. In contrast, histological sections of the colons in the L-MAN-ROSI group showed markedly reduced inflammation with only mild inflammatory infiltration, edema and normal bowel wall thickness (Fig. 4H). Histology scoring based on HE-stained picture also concluded that the score of L-MAN-ROSI-LP was lower than that of the ROSI and model groups (Fig. 4I).

Myeloperoxidase (MPO) was an enzyme presented in a variety of immune- and inflammation-related cells, and its activity was proportional to the degree of inflammation in the tissue. Decreased MPO activity in inflamed tissue was a sign of tissue repair and healing. The MPO activity of each mouse colon tissue was measured and shown in Fig. 4G. Treatment with ROSI and MAN-ROSI-LP significantly reduced the DSS-induced MPO enzyme activity in colon tissue, and L-MAN-ROSI-LP existed the better efficacy compared with ROSI. This phenomenon revealed that L-MAN-ROSI-LP system could effectively deliver the drug to the inflammatory site and exert better therapeutic efficacy than free drug at the same dose.

IBD was featured with persistent and recurring inflammation, during which, the misfunction of macrophage population played a dominant role. In DDS-induced colitis mice model, a large number of pro-inflammatory macrophages and monocytes infiltrated in mucosa to triggered inflammatory and immune responses [29]. Therefore, macrophage was the appropriate and effective target for IBD therapy [30]. Existing drugs, including classic non-steroidal anti-inflammatory drugs, glucocorticoids, antibody drugs and synthetic immunosuppressants were related to regulate intestinal macrophage differentiation and activity [31–33]. Due to the systemic side effects and the long course of treatment, there was still no approved drug system for targeting inflammatory macrophages as pharmaceutical product. Mannosylated liposomes specifically targeting to macrophages was an effective way for IBD treatment. Liposome was used as carrier for drug delivery with higher biocompatibility and ROSI as the agonist of PPAR-γ was act as model drug. Drug or delivery system was injected *via* tail vein that would facilitate the treatment of deep inflammation without inhibiting

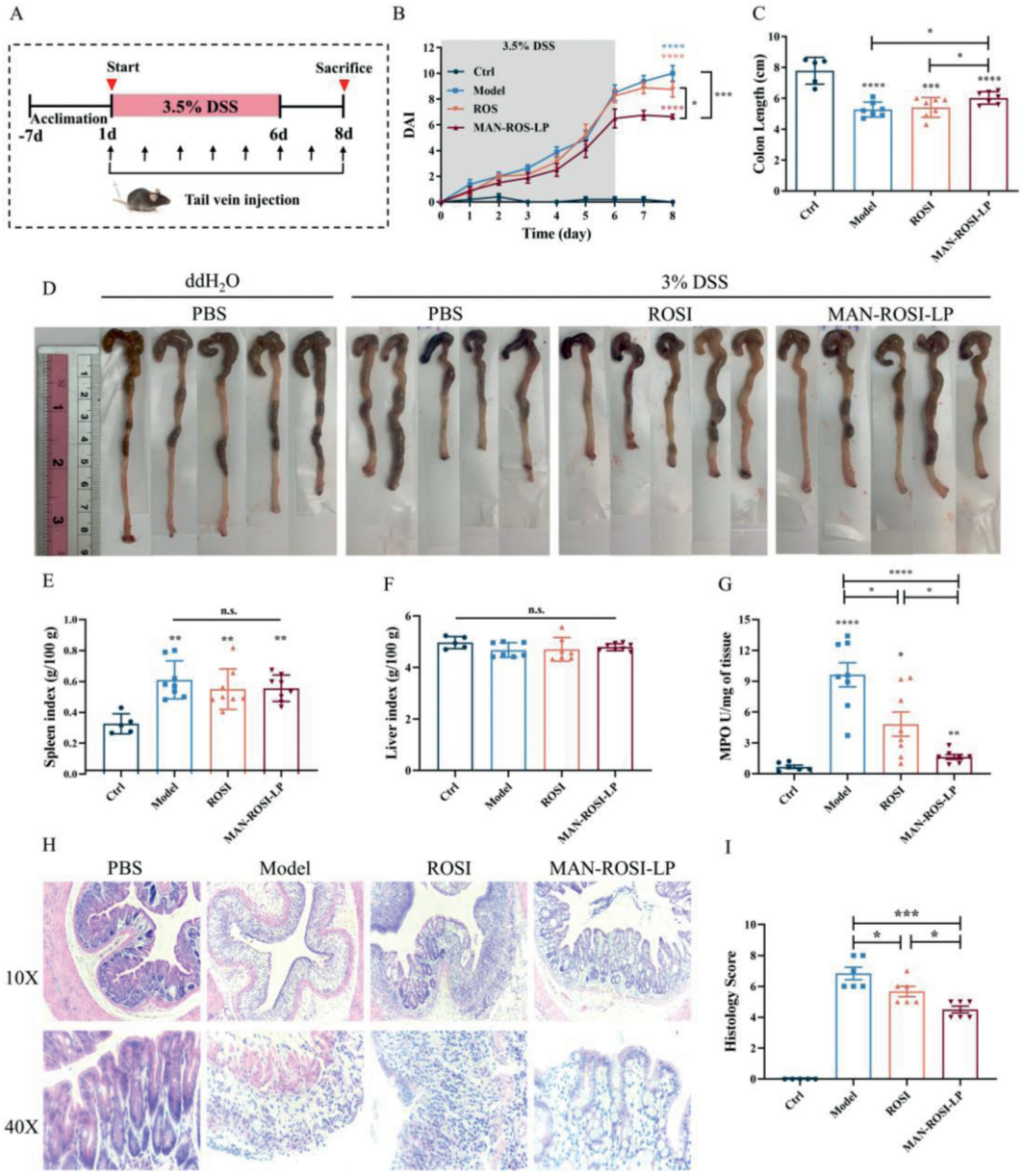

Fig. 4. Anti-inflammatory effect of MAN-ROSI-LP in DSS induced mice model. (A) The timeline of liposome treatment *in vivo*. C57BL/6 mice were freely fed with 3.5% DSS for 6 days to induce IBD, and then changed to drinking water. 100 μL PBS, 0.2 mg/kg ROSI or MAN-ROSI-LP with 0.2 mg/kg ROSI were injected into the tail vein every day. (B) Mice were weighed daily, and DAI was assessed. (C, D) At the end of the study (day 8), the length of mouse colons were measured, and colon tissue were collected for image. (E, F) The spleens and livers of mice were weighed. (G) MPO activity of colon tissue were detected. (H, I) Colon tissue was taken for HE staining and histological scoring. All significant differences of MAN-DiI-LPs compared with PEG-DiI-LP were determined by one-way ANOVA, data represent mean ± SD (n.s. means not statistically different, $^{*}P < 0.05$, $^{**}P < 0.01$, $^{***}P < 0.001$, $^{****}P < 0.0001$).

repair of mucosal damage and ulcer. It also avoided the impact of the complex intestinal environment and act on macrophages directly. Furthermore, particle size was also screened to realize the best macrophage targeting. It was a significant improvement of therapeutic effect than free drug with a very low drug concentration in the IBD mouse model.

MR was a neutral receptor for mannose that expressed on the surface of macrophages and was closely related to the functions of the innate immune system and homeostasis. This study confirmed that compared to PEG-LP, MAN-LP with the same particle size displayed better targeting efficiency to cultured macrophage RAW 264.7, but not epithelial cell A549 *In-vitro*. Furthermore, L-MAN-LPs had the better ability to target macrophages of the model organism zebrafish and intestinal inflamed areas of IBD mice model. Moreover, the combination of mannose and MR would play a role in inhibiting the secretion of inflammatory factors by macrophages and further attenuating the inflammatory response of the intestine. Therefore, mannose modification was an effective way to deliver the drug to inflammatory macrophages and exert the medicinal effect.

Except the specific ligand-receptor combination, particle size was an important parameter for targeting inflammatory lesions. Previous studies confirmed that the larger liposome particles were more efficiently taken up than smaller one, while they were more likely to be trapped by splenic macrophages when the particle size was greater than 400 nm [34,35]. The MAN-LPs were prepared with different size from 100 nm to 300 nm, and the macrophage targeting efficiency was investigated individually. With the size increased, the uptake of MAN-LPs by macrophage and accumulation of MAN-LPs in inflammatory bowel sites were significantly in-

creased. One of the mechanisms could be that macrophage preferentially recognized and uptake the larger sized particles. On the other hand, with the diameter increased, more mannose molecules can be decorated on the surface of liposomes for macrophage targeting enhancement [36]. In addition, a previous study claimed that the diameter of fenestrated endothelium within the liver sinusoidal was between 100 nm and 150 nm, which facilitated the hepatocytes uptake for the particles smaller than this size [37]. Therefore, liposomes with larger particle size could escape from the entrapment of the liver sinusoids.

ROSI was reported to be benefit for IBD model by alleviation of activated intestinal macrophages [38]. It was expected to bind to PPAR-γ expressed on activated macrophages to inhibit the inflammatory response and repair the mucosa. In this research, the ability of MAN-ROSI-LPs alleviating LPS-induced secretion of pro-inflammatory factors in macrophages was particle size dependent. In DSS-induced IBD mice model, L-MAN-ROSI-LPs treatment significantly ameliorated the changes of symptoms, pathological manifestations and tissue MPO activity with a very low drug dose that did not produce significant benefits in free drug group. It was an easy and efficient delivery system that increased the accumulation of ROSI in the inflammatory sites for IBD treatment.

The potential toxicity of the delivery system was also an important issue to consider. There were already a variety of liposomes in the pharmaceutical market for the treatment of diseases such as cancer and influenza, which reflected the excellent biological safety of liposomes in clinic. Our results showed that tail vein injection of MAN-ROSI-LP for short term did not significantly change the liver and spleen indices of IBD mice. Moreover, the DSS-induced spleen index increasing was reduced due to the potent effect of the drug, indicating good biocompatibility of this targeted drug delivery systems.

In conclusion, different sized mannose-modified ROSI loaded liposomes were synthesized and successfully targeted to macrophages on both *in-vitro* and *in-vivo* zebrafish and mice models. The enhanced targeting effect and anti-inflammatory effect of MAN-ROSI-LPs was size-dependent, which was also well confirmed in the zebrafish and intestinal inflammation site of IBD mice model without observed toxicity. Using MR as a targeting receptor and mannose-modified liposomes with particle size tailing as the drug delivery systems may provide an effective strategy for macrophage-targeting to deliver lipophilic drugs, which can enhance IBD therapeutic activity and minimize the systemic adverse effects of the drug.

Declaration of competing interest

The authors declare that they have no known competing financial interests or personal relationships that could have appeared to influence the work reported in this paper.

Acknowledgments

This work was supported by research grants from the Macau Science and Technology Development Fund (No. 0086/2021/A2), Shenzhen Fundamental Research Program (No. SGDX20210823103804030), the 2020 Guangdong Provincial Science and Technology Innovation Strategy Special Fund (Guangdong-Hong Kong-Macau Joint Lab, No. 2020B1212030006), and Guangdong Basic and Applied Basic Research Foundation (No. 2022A1515012416). We thank the members of the FHS Animal Facility at the University of Macau for their experimental and technical support, and thank Prof. We Ge for the support of zebrafish breeding and injection.

Supplementary materials

Supplementary material associated with this article can be found, in the online version, at doi:10.1016/j.cclet.2023.108361.

References

[1] S.C. Ng, Gastroenterol. Hepatol. 12 (2016) 193–196.
[2] G.G. Kaplan, J.W. Windsor, Nat. Rev. Gastroenterol. Hepatol. 18 (2021) 56–66.
[3] D.C. Baumgart, W.J. Sandborn, Lancet 369 (2007) 1641–1657.
[4] K.J. Maloy, F. Powrie, Nature 474 (2011) 298–306.
[5] T. Kobayashi, B. Siegmund, C.L. Berre, et al., Nat. Rev. Dis. Prim. 6 (2020) 74.
[6] R. Ungaro, S. Mehandru, P.B. Allen, et al., Lancet 389 (2017) 1756–1770.
[7] M.C. Sun, W.Y. Ban, H. Ling, et al., Chin. Chem. Lett. 33 (2022) 4449–4460.
[8] P. Liu, C.F. Gao, H.G. Chen, et al., Acta Pharm. Sin. B 11 (2021) 2798–2818.
[9] S. Barua, S. Mitragotri, Nano Today 9 (2014) 223–243.
[10] A.A. Date, G. Halpert, T. Babu, et al., Biomaterials 185 (2018) 97–105.
[11] X.D. Zhang, X. Zhao, S.S. Tie, et al., J. Control. Release 342 (2022) 372–387.
[12] A. Aprodu, J. Mantaj, B. Raimi-Abraham, et al., Pharmaceutics 11 (2019) 127.
[13] J.Q. Xu, T.J. Chu, T.T. Yu, et al., ACS Nano 16 (2022) 13037–13048.
[14] W.S. Garrett, J.I. Gordon, L.H. Glimcher, Cell 140 (2010) 859–870.
[15] K.T. Magar, G.F. Boafo, M. Zoulikha, et al., Chin. Chem. Lett. 34 (2023) 107453.
[16] W. He, N. Kapate, C.W. Shields 4th, et al., Adv. Drug Deliv. Rev. 165 (2020) 15–40 -166.
[17] H. Nakase, K. Okazaki, Y. Tabata, et al., J. Gastroenterol. 38 (2003) 59–62.
[18] N. Watanabe, K. Ikuta, K. Okazaki, et al., Digest. Dis. Sci. 48 (2003) 408–414.
[19] R. Hontecillas, W.T. Horne, M. Climent, et al., Mucosal. Immunol. 4 (2011) 304–313.
[20] J.D. Ramakers, M.I. Verstege, G. Thuijls, et al., J. Clin. Immunol. 27 (2007) 275–283.
[21] H.L. Liang, Q. Ouyang, World J. Gastroenterol. 14 (2008) 114–119.
[22] S.E. Nissen, K. Wolski, New Engl. J. Med. 357 (2007) 100.
[23] M.L. Thomas, S.J. Lloyd, Ann. Pharmacother. 35 (2001) 123–124.
[24] F.H. Deng, S.Y. He, S.D. Cui, et al., J. Crohns Colitis 13 (2019) 482–494.
[25] U. Gazi, L. Martinez-Pomares, Immunobiology 214 (2009) 554–561.
[26] Y.J. Song, Y.Q. Huang, F. Zhou, et al., Chin. Chem. Lett. 33 (2022) 597–612.
[27] C.A. MacRae, R.T. Peterson, Nat. Rev. Drug Discov. 14 (2015) 721–731.
[28] B. Chassaing, J.D. Aitken, M. Malleshappa, et al., Curr. Protoc. Immunol. 104 (2014) 15 25.1-15.25.14.
[29] E. Zigmond, C. Varol, J. Farache, et al., Immunity 37 (2012) 1076–1090.
[30] Y.R. Na, M. Stakenborg, S.H. Seok, et al., Nat. Rev. Gastroenterol. Hepatol. 16 (2019) 531–543.
[31] J. Ehrchen, L. Steinmuller, K. Barczyk, et al., Blood 109 (2007) 1265–1274.
[32] H. Bantel, C. Berg, M. Vieth, et al., Am. J. Gastroenterol. 95 (2000) 3452–3457.
[33] A.C. Vos, M.E. Wildenberg, I. Arijs, et al., Inflamm. Bowel Dis. 18 (2012) 401–408.
[34] C.D. Walkey, J.B. Olsen, H.B. Guo, et al., J. Am. Chem. Soc. 134 (2012) 2139–2147.
[35] S. Chono, T. Tanino, T. Seki, et al., J. Pharm. Pharmacol. 59 (2007) 75–80.
[36] A. Chakrabarti, S. Podder, Biochim. Biophys. Acta 1024 (1990) 103–110.
[37] E. Wisse, F. Jacobs, B. Topal, et al., Gene Ther. 15 (2008) 1193–1199.
[38] A.Z. Mirza, I.I. Althagafi, H. Shamshad, Eur. J. Med. Chem. 166 (2019) 502–513.